GeoAmericas2020
4th PAN AMERICAN CONFERENCE ON GEOSYNTHETICS
26-29 APRIL 2020 • RIO DE JANEIRO • BRAZIL

Performance of Roadways with Enhanced Lateral Drainage (ELD) Geotextiles to Mitigate Detrimental Effects of Moisture Migration

A. El Hachem, Geotechnical and Tunneling, WSP USA, Austin, TX, USA.
J.G. Zornberg, Department of Civil Architectural and Environmental Engineering, The University of Texas at Austin, Austin, TX, USA.

ABSTRACT
Moisture increase in the subgrade and base layers of a pavement section is one of the main causes for its premature distress and failure. Infiltration, capillary rise and lateral moisture transfer constitute the major sources of the increased water content. An investigation was conducted with the objective of mitigating the severe effects of increased moisture by installing a geotextile with enhanced lateral drainage (ELD) characteristics in pavements subject to capillary rise from a high-water table. Specifically, an accelerated pavement-testing program was conducted at The University of Texas at Austin laboratories to assess the benefits of an ELD geotextile in decreasing the moisture in the pavement layers and thus improving its performance. A Model Mobile Load Simulator (MMLS3) device was used to load a six-foot by six-foot by one-foot pavement section consisting of kaolinite subgrade and unbound base. A hydraulic system was designed to establish a constant water level in the pavement and allow for capillary rise in the subgrade and base layers. Three different configurations were tested with ELD and conventional geotextiles installed at the subgrade and base interface. The configurations were initially evaluated hydraulically through the evaluation of column tests constructed using the same configuration of soils and geotextiles to be constructed in the MMLS3 device. The pavement performance was assessed by monitoring changes in volumetric moisture content, particle movements, and pavement rutting. The test results showed that installing the ELD geotextile improved the pavement performance, highlighting the effectiveness of the ELD geotextile in draining the extra moisture and reducing distresses.

1. INTRODUCTION

Due to the variation of the environmental conditions, the resilient moduli of the pavement layers vary with the changes in moisture content. Moisture increase can affect the soil in two ways resulting in a decrease in its resilient modulus: It alters the state of stresses and breaks the cementation between the soil particles (ARA Inc. 2000). The change in the matric suction due to the change in moisture levels affects the state of stresses in a soil layer and consequently its resilient modulus (Fredlund et al.1977). The pavement layers are generally constructed at a moisture level close to the optimum value for compaction; however, the moisture conditions fluctuate after interacting with the surrounding environment. Moisture can be supplied to the different pavement layers through any of the following mechanisms: capillary rise from a shallow phreatic surface, infiltration through pavement cracks and shoulders, lateral moisture transfer, and frost-thaw action (Azevedo, 2016; Sarlour. 2015). The moisture in the pavement section is generally present under unsaturated conditions and, therefore, not easy to drain due to the high suction gradients. An innovative geotextile with enhanced lateral drainage (ELD) characteristics is installed within the pavement structure to mitigate the effects of the excess moisture by wicking away water from the unsaturated soil voids.

Enhanced lateral drainage is achieved by incorporating the wicking fiber technology within a woven geotextile resulting in an innovative product that can fulfill the functions of reinforcement, separation, and drainage under unsaturated conditions (Zornberg et al., 2017). The wicking fibers are made of nylon and oriented in the intended drainage direction. They are formed of hygroscopic material with the ability to attract and wick water. The nylon fibers are manufactured with a special cross section forming tiny channels that conduct water. Figure 1 shows the grooved cross section of the wicking fibers with the water transport mechanism through the tiny tubes (Azevedo, 2016).

Figure 1. Wicking Fiber Cross Section

The effectiveness of the ELD geotextile can be verified by comparing the performance of two pavement test sections subject to moisture increase with and without an ELD geotextile. However, this alternative turns out to be expensive and time prohibitive. Moreover, the full scale in-situ section is subject to several environmental variables that makes it difficult to isolate the intended differences between the test and control configurations. Also, field monitoring is always accompanied with numerous limitations and difficulties. Alternatively, the ELD system can be tested in a lab environment where there is a better control over the variables. The laboratory test would allow for a superior monitoring program and produce the results in a timely manner.

Therefore, an accelerated pavement test using a Model Mobile load Simulator (MMLS3) was established to assess the advantages of installing an ELD geotextile in a pavement section subject to moisture increase from a shallow water table. This paper presents the design and development of the laboratory testing program at the University of Texas at Austin laboratories

2. ACCELERATED PAVEMENT TESTING

2.1 Test Setup

A third scale Model Mobile Load Simulator (MMLS3) was used to simulate traffic passes on 6ftx6ft laboratory pavement sections. This study aims at evaluating the performance of roadways with ELD geotextiles as compared to conventional sections rather than simulating real pavement performance. Therefore, the pavement sections are designed to reach failure in a reasonable amount of time. The section was constructed in a 6ftx6ftx1ft test box made of steel plates. The pavement consisted of a 6-inch fine grained subgrade overlain by 5 inches of unbound base and 1 inch of hot mix asphalt. A geotextile was installed at the interface of the subgrade and base layers with its ends extended out of the test box to allow for potential lateral moisture drainage. The test section is illustrated in Figure 2.

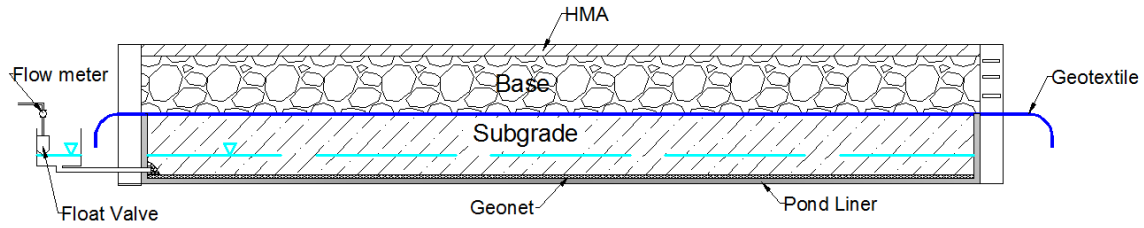

Figure 2. Test Setup Cross Section

In this test, the excess moisture was supplied to the pavement through capillary rise from a constant water table. A hydraulic system was designed to maintain a constant water level throughout the test. This was achieved by connecting the box to an external water container having a constant head equal to the desired water table elevation. The head in the container was controlled by a float valve, and a water meter was installed to measure the water supply to the pavement section. The water was supplied to a geonet installed at the base of the box to ensure uniform water rise in the subgrade layer. A pond liner was placed in the box to provide a watertight system.

2.2 *Materials*

The subgrade layer consisted of fine-grained soil that possesses a high capillary rise potential and exhibits a significant decrease in its resilient modulus with an increase in its moisture content. Since the water supply to the system is through capillary rise in the subgrade layer, this material should have a comparatively high permeability to minimize testing duration. Therefore, kaolinite clay was selected as the subgrade layer. This material has been widely used in laboratory testing with numerous tests performed with this type of soil at The University of Texas laboratories (Daniel et al. 1992). This commercially available material possesses well known properties over time. The Kaolin used in this study is an English Clay mined from Cornwall in the United Kingdom and available under the commercial name of Grolleg Kaolin from IMERYS Company. Standard proctor compaction tests were performed on this clay per ASTM D698-12e2. The maximum dry density was 86.5 lb/ft^3 at a moisture content of 28%.

Cemex Flexible Base Gravel dredged from the Balcones Quarry south of New Braunfels, TX, USA was used as the base material. This soil was classified as Silty Clayey Gravel (GC-GM) as per ASTM D 2487. Results from grain size distribution showed the presence of 16% fines in this base material. This relatively high fines content in the base material is advantageous for this test since it increases the potential of moisture rise to the base layer. Standard Proctor tests

were performed on this material, and the results were corrected for oversize particles based on ASTM D4718/D4718M-15. The maximum dry density was 135 lb/ft^3 at a moisture content of 7.5%.

The geotextile with enhanced lateral drainage capabilities used in this study was the Mirafi H2Ri woven geotextile. The control product was the Mirafi RS380i. The two geotextiles exhibit similar tensile strengths and stiffness with the main difference being the lateral drainage capabilities.

2.3 *Instrumentation*

Three main criteria were evaluated to assess the pavement performance in each test:

- Rutting at a given loading cycle using a laser profilometer mobilized on an aluminum frame.
- Particle movement within the base layer using linear potentiometers (LPs) connected to tell-tales via cobalt based alloy wires.
- Volumetric moisture content of the subgrade and base material using Decagon EC-5 capacitance probes.

2.4 *Hydraulic Assessment*

A hydraulic study of the proposed pavement configuration was conducted before performing the accelerated pavement test. The objective of this study was to quantify the moisture increase in the different pavement layers due to capillary rise from a nearby water table and to assess the effect of the wicking geotextile on this water rise in the system. The testing procedures followed to achieve these objectives are described by El Hachem and Zornberg, 2019. The same kaolinite subgrade and Cemex base material were compacted and subjected to a constant water table in a small-scale test box. As shown in Figure 3, a vertical and horizontal array of time domain reflectometers (TDRs) were installed to monitor the volumetric moisture content throughout the testing period. A geotextile was installed between the subgrade and base layers and extended out of the box to allow for lateral moisture drainage, if any.

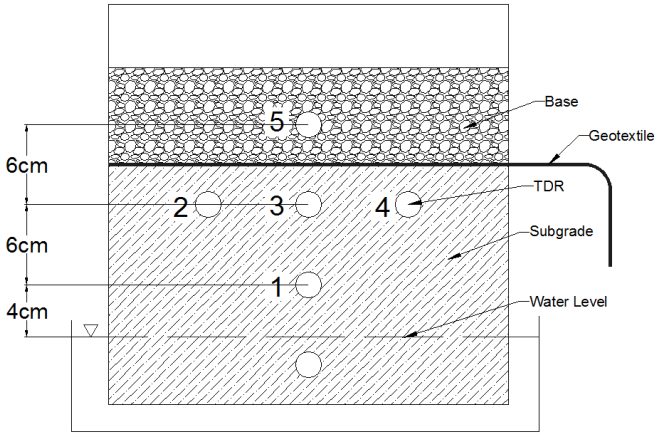

Figure 3. Constant Water Table Test Setup

Four configurations were tested for the hydraulic performance to verify the expected moisture trends before running the MMLS3 tests. A test with no geotextile was first performed to determine the capillary rise rate and extent in the subgrade and base materials. Subsequent tests with standard woven geotextiles and ELD geotextiles were performed with the tip of the fabric extended out of the box and wrapped in a zip lock bag to collect any moisture exiting from the system. A different configuration was also tested where a nonwoven geotextile was installed on top of the ELD geotextile.

The detailed results of the hydraulic assessment are presented in El Hachem and Zornberg, 2019. The performed constant water table tests demonstrated the ability of the ELD geotextile to laterally drain moisture out of the pavement layers in the system. This was shown by the presence of water in the extended portion of the geotextile and the lower moisture readings in the TDRs for the tests employing the ELD geotextile.

2.5 *MMLS3 Testing Procedures*

The MMLS3 testing procedures comprised of four main steps: material preparation, pavement construction, loading and distress measurement, and test dismantling.
Proper material preparation was crucial to achieve similar conditions among the different performed tests. Kaolinite clay was purchased in 55 lb. powder bags and moisture conditioned in the lab to about 25% gravimetric moisture content. A spray pump was used to slowly add water to the clay in a concrete mixer. The base material was air dried and then moisture conditioned to around 7.5% gravimetric moisture content. The prepared subgrade and base material were stored in sealed drums to preserve their moisture state.

The test box was then assembled with the pond liner and geonet placed at its base. The kaolinite subgrade was compacted in three lifts to 85% relative compaction in relation to the maximum dry density as determined by the standard proctor test. After each lift, the surface of the soil was scarified to hydraulically connect the entire subgrade layer. The Decagon EC-5 moisture sensors were installed in horizontal arrays of three sensors at two elevations 2 inches and 4 inches below the geotextile. After compacting the subgrade layer, the geotextile was installed with its ends extended out of the box. Although, lateral moisture drainage was only expected for the cases with the ELD geotextile, the conventional geotextiles were also extended out of the box to maintain a similar test configuration. The base layer was also compacted in three lifts to 85% relative compaction in relation to the determined maximum dry density. For the base layer, moisture sensors were installed in horizontal arrays of two sensors at two elevations 2 inches and 4 inches above the geotextile. Figure 4 shows a cross section of the test box with the location of the volumetric moisture content sensors numbered from 1 to 10.

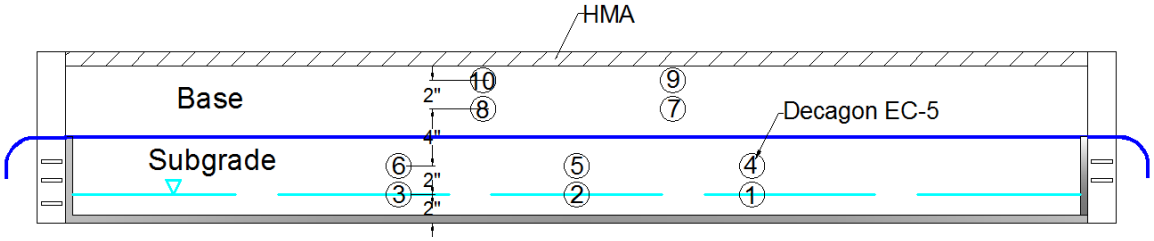

Figure 4. Volumetric Moisture Content Sensor Configuration

A total of ten tell-tales were installed in the base layer at 2 inches and 4 inches above the geotextile with 5 sensors at each elevation as shown in Figure 5. The Linear potentiometers connected to the tell-tales are numbered from zero to nine as shown in the below figure.

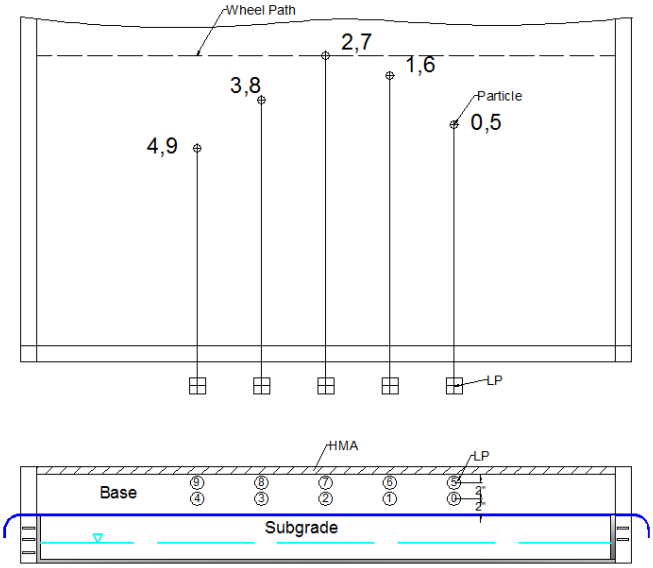

Figure 5. Linear Potentiometer Configuration

After constructing the subgrade and base layers, Hot Mix Asphalt material was spread over the section and compacted via a gas vibratory force plate compactor. One white stripe in the longitudinal direction and three stripes in the transverse direction were painted on top of the pavement to provide a bright reflective surface for the laser used for rutting measurement. Figure 6 shows the pavement section with the location and nomenclature of the rutting profiles.

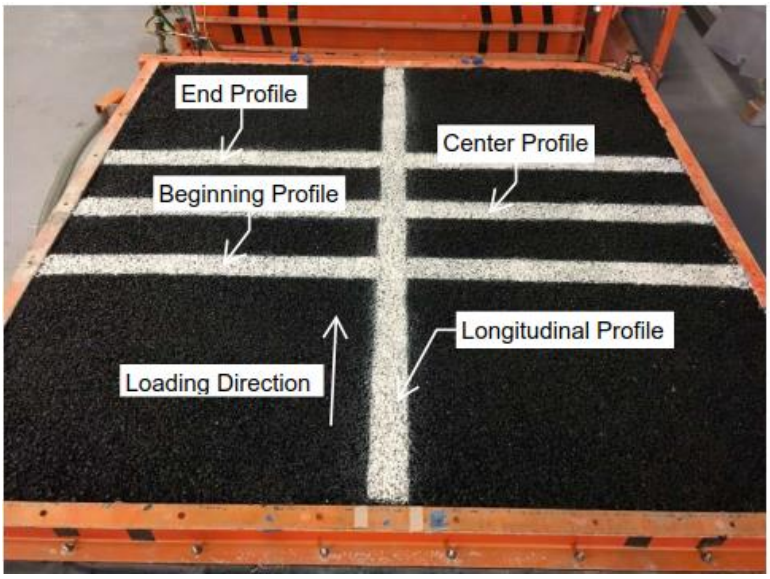

Figure 6. Paved MMLS3 Test Section

The pavement was then connected to the hydraulic system where the water level in the container was maintained at 2 inches above the base of the test box. The water was allowed to rise in the pavement layers while monitoring the volumetric moisture content increase in the system.

After hydraulic equilibrium was reached, an initial profile was taken for the four transverse and longitudinal sections to establish the baseline sections. The Model Mobile Load Simulator (MMLS3) was then mounted over the pavement. The machine has four 300 mm diameter single wheels equipped with a suspension system that ensures the independence of the wheel load from the displacement up to 20 mm. The pneumatic tires were inflated to 700 kPa resulting in a wheel load equal to 2700 Newton. The machine was set to 6000 cycles/hour. A loading program was established, and rutting profiles were measured after each set of loading cycles.

The section was loaded until excessive distress was witnessed. A cut through the failed pavement was made to visually examine the rutting propagation through the pavement layers and interpret the failure mechanisms. The material was finally removed from the test box, and samples were retrieved for gravimetric moisture content measurement. The test box was then prepared for the next test.

2.6 Testing Program and Example Results

Based on the hydraulic assessment outlined in Section 2.4, three main test configurations were planned to verify the results obtained from the constant water table test in the small-scale box: conventional GT, ELD GT, and ELD GT overlain by nonwoven GT. Multiple repeat tests of the same configuration were planned as part of this testing program to verify the test results. The testing program is currently in progress at The University of Texas Accelerated Pavement Testing facilities. In this section, results from an MMLS3 test with ELD GT overlain a nonwoven geotextile are discussed in detail.

Five loading stages were performed, and rutting measurements with the laser profilometer were conducted after each stage:

- Stage 1: 0 to 100 passes
- Stage 2: 100 to 1,000 passes
- Stage 3: 1,000 to 3,000 passes
- Stage 4: 3,000 to 10,000 passes
- Stage 5: 10,000 to 15,000 passes

The rutting profiles after each loading stage for the longitudinal and transverse center sections are presented in Figure 7 and Figure 8, respectively. The plots show the surface pavement deflection in relation to the initial surface profile. About 18 mm rutting was measured after 10,000 wheel passes. The pavement failure criteria per the MEPDG design guide is 0.5 inch (12.7 mm) of rutting. Therefore, the pavement in this test failed between 3,000 and 10,000 wheel passes. The pavement was then loaded with an additional 5,000 cycles until excessive plastic deformation was witnessed.

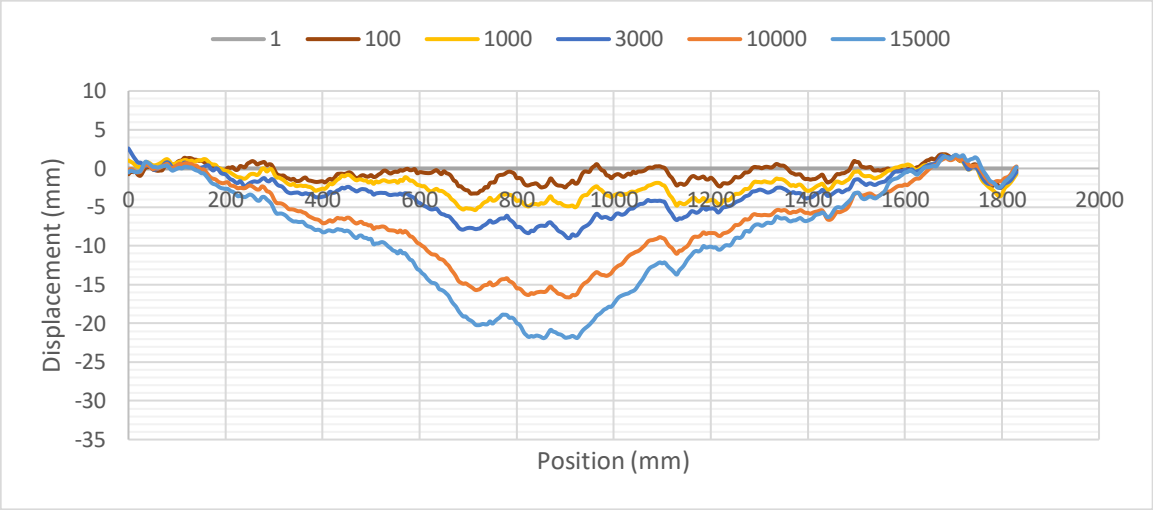

Figure 7. Longitudinal Rutting Profile

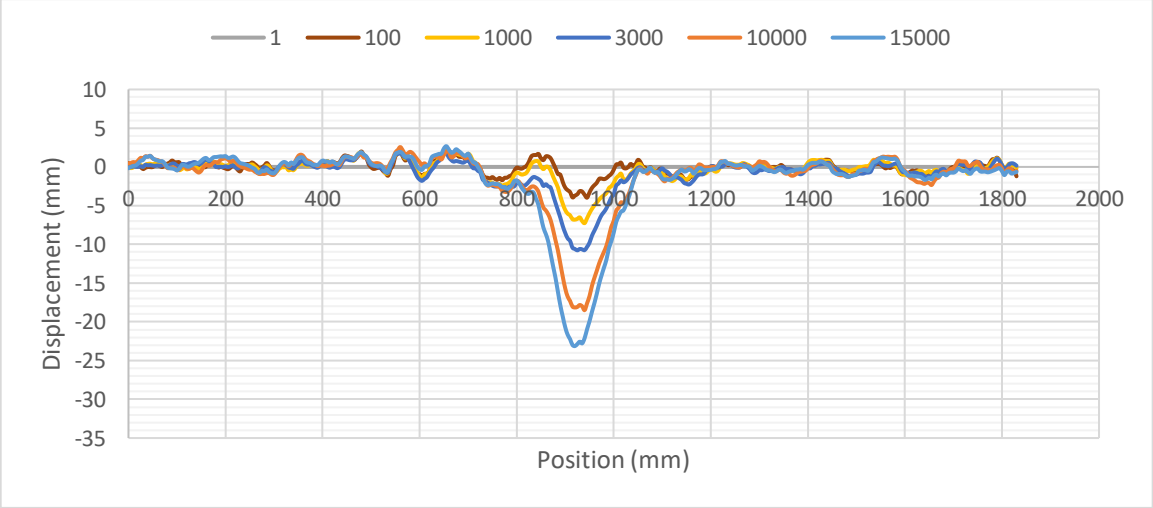

Figure 8. Transverse Center Rutting Profile

Particle movements were monitored at 10 locations in the base layer as shown in Figure 5. The results show that the closest particles to the wheel path exhibited the most movement. Minimal deformation was recorded for the particles farther than 9 inches from the wheel path. The rutting mechanism resulted in some particles moving towards the wheel path due to the excessive plastic settlement under wheel loading. Moreover, in this test, moisture was observed at the geotextile ends that were extended out of the pavement box indicating that lateral drainage was taking place.

After finishing the test, a cross section perpendicular to the loading direction was taken at the center of the pavement to visualize the rutting propagation through the different pavement layers as shown in Figure 9. The picture shows the plastic deformation in both the base and subgrade layers. Lateral flow rutting is apparent in the depression under the wheel path accompanied by shear upheaval on either side of the depression. A manual measurement of the rutting on top of the geotextile indicated about 14 mm movement in the clay subgrade.

Figure 9. Pavement Cut Section Photos

3. CONCLUSIONS

A hydraulic study was conducted to assess the ability of the ELD geotextile to drain water from a pavement structure subject to moisture increase from a shallow water table. The constant water table test performed on three different geotextile configurations showed a lower moisture content in the setups employing the ELD geotextiles. An accelerated pavement testing program was developed at The University of Texas laboratories to assess the performance of roadways with the ELD geotextile and verify the results of the hydraulic assessment. A Model Mobile Load Simulator (MMLS3) was used to load a pavement section formed of fine-grained subgrade and unbound base material. An instrumentation program was developed to monitor the moisture content in the system and measure the pavement distress throughout the test. The performed tests thus far demonstrated the ability of the designed experimental setup to assess the performance of the pavement with a certain geotextile configuration. It also permitted the determination of the failure mechanisms and the percentage of distress in each of the pavement layers. The obtained results so far complemented the hydraulic test study through similar volumetric moisture trends and observed moisture drainage in the extended ELD geotextile ends. The decreased moisture in the system will be reflected in the mechanical performance of the pavement. The testing program is currently in progress where multiple tests of each configuration are being performed to verify the findings.

ACKNOWLEDGEMENTS

The authors appreciate the support provided by TenCate Geosynthetics to this research, which is gratefully acknowledged.

REFERENCES

ARA Inc. (2000). Appendix DD-1: Resilient modulus as a function of soil moisture – summary of predictive models, *Guide for the Mechanistic Empirical Design of New and Rehabilitated Pavement Structures,* Transportation Research Board National Research Council.

ARA Inc. (2004). Part 3. Design analysis: Chapter 3. Design of new and reconstructed flexible pavements. *Guide for the Mechanistic Empirical Design of New and Rehabilitated Pavement Structures,* Transportation Research Board National Research Council.

ASTM D 2487-17. Standard Practice for Classification of Soils for Engineering Purposes (Unified Soil Classification System), *American Society of Testing and Materials,* West Conshohocken, Pennsylvania, USA.

ASTM D 4719/D4718M-15. Standard Practice for Correction of Unit Weight and Water Content for Soils Containing Oversize Particles, *American Society of Testing and Materials,* West Conshohocken, Pennsylvania, USA.

ASTM D 698-12e2. Standard Test Methods for Laboratory Compaction Characteristics of Soil Using Standard Effort (12400 ft-lb/ft^3 (600 kN-m/m^3)), *American Society of Testing and Materials*, West Conshohocken, Pennsylvania, USA.

Azevedo, M. (2016). Performance of geotextiles with enhanced drainage, *Doctoral Dissertation.* The University of Texas at Austin, Austin, TX, USA.

Daniel, D.E., Burton, P.M., and Hwang, S.D. (1992). Evaluation of four vadose zone probes used for leak detection and monitoring, *Current Practices in Ground Water and Vadose Zone Investigation,* ASTM STP 1118, Philadelphia, PA, USA.

Decagon Devices (2012). *EC-5 Soil Moisture Sensors User Manual (Version 1).* Pullman, WA: Decagon Devices, Inc.

El Hachem, A. and Zornberg, J.G. (2019). Enhanced lateral drainage geotextile to mitigate the effects of moisture migration from a high water table, *Geo-Congress 2019*, Philadelphia, PA, USA, 227-234.

Fredlund, D.G., Bergan A.T., and Wong P.K. (1977). Relation between resilient modulus and stress conditions for cohesive subgrade soils, *Transportation Research Record 642*, TRB, National Council, 1977. Washington, D.C., USA, pp. 73-81.

Sarlour, F. (2015). Moisture influence on structural behavior of pavements, *Doctoral Dissertation,* KTH Royal Institute of Technology, Stockholm, Sweden.

Zornberg, J.G., Azevedo, M., Sikkema, M., and Odgers, B. (2017). Geosynthetics with enhanced lateral drainage capabilities in roadway systems. *Transportation Geosynthetics,* 12, 80-100. Doi: 10.1016/j.trgeo.2017.05.008.